Spontaneous formation of hybrid heterotrimer of Fe_3O_4-Ag_2S-ZnS by seeded-growth method

Shaghraf Javaid[a], Wei Chen[a], Guohua Jia[a] and Franca Jones[a]**

a Curtin Institute of Functional Molecules and Interfaces, School of Molecular and Life Sciences Curtin University, Bentley, Perth WA, 6102, Australia

Email: F.Jones@curtin.edu.au, guohua.jia@curtin.edu.au

Three-component containing hybrid heterostructures with multiple functionalities are highly desirable but difficult to synthesize. Herein, we have demonstrated the utilization of simple seeded-growth approach for the synthesis of a hybrid heterotrimer of iron oxide-silver sulfide-zinc sulfide (Fe_3O_4-Ag_2S-ZnS). At first, Fe_3O_4-Ag was synthesized by using silver nanoparticles (Ag NPs) as a seed followed by its *in-situ* sulfurization to produce a dimer of Fe_3O_4-Ag_2S. This dimer was successively used as a seed under controlled experimental conditions for the synthesis of Fe_3O_4-Ag_2S-ZnS. The availability of such trimers through this approach can shed some light on the integration of entirely different functionalities in one-particle systems.

Introduction

Recent investigations suggest that hybrid heterostructures, which are composed of more than one component, have become an attractive candidate for a number of applications i.e. catalysis, biomedicine, dye degradation, electrochemical applications, photodetectors, bio-labelling and so on.[1-8] Its popularity is generally associated with its multifunctionality, which essentially means that all of its individual components retain their original identities with some additional unique properties as a result of synergistic effects.[9-12] Although many efforts have been directed towards the synthesis of sophisticated hybrid nanomaterials as yet only two-component (dimers) models remain the most understood.[13] This is due to the lack of a complete mechanistic understanding of the process, the uncertainty associated with side products and the nature of the participating constituents.[6, 14, 15] To some extent, such complexities can be reduced by choosing a simple synthesis approach i.e. a seeded-growth method.[16] Recently, Javaid *et al*.[15] has reported the formation of well-defined high order hybrid heterotrimer of Fe_3O_4-Au-CdS by a two-step approach where Fe_3O_4-Au dimer was used as a seed for the subsequent growth of CdS. Inspired by this work, herein we report the successful formation of a hybrid heterotrimer of Fe_3O_4-Ag_2S-ZnS which integrates three different functionalities in a single particle i.e. magnetic, optical and semiconducting properties.

Among others, transition metal sulfides (TMSs) remain the most favourite candidate for hybrid nanomaterials i.e. CdS, Fe_7S_8, ZnS, NiS, CoS etc.[17] The reason behind this interest lies in their exceptional catalytic performance. Extensive studies have revealed the promising potential of Ag_2S-ZnS based hybrid heterostructures, attributed to their photoluminescence (PL) and optical properties.[4, 18-20] However, to the best of our knowledge, incorporation of a magnetic entity in such a system under controlled experimental conditions has never been reported before. Therefore, in this paper we have used Fe_3O_4-Ag_2S dimer as a seed for the heterogeneous nucleation of ZnS, yielding a sophisticated trimer of Fe_3O_4-Ag_2S-ZnS. Such efforts can widen the synthetic "palette" of three-component containing hybrid nanomaterials and therefore can be desirable to provide insights for the future development of hybrid heterotrimers.

Experimental

Materials

Silver acetate (Ag(OAC), 99 %), oleylamine (OL-Am, 70), 1-octadecene (ODE, 90 %), oleic acid (OA, 90 %), dodecanethiol (DDT, 98 %), iron acetylacetonate ($Fe(acac)_3$, 99.9 %), sulphur (S, 99.99 %) and zinc nitrate hexahydrate ($Zn(NO_3)_2.6H_2O$, 99.0 %) were purchased from Sigma-Aldrich. All chemicals were used as received without further purification.

Synthesis of Fe_3O_4-Ag

The heterodimer of Ag-Fe_3O_4 was synthesized according to the literature method.[21, 22] At first, $Fe(acac)_3$ was used to generate iron oleate *in-situ* in the presence of oleic acid and OL-Am. In a typical reaction, 50 mg of $Fe(acac)_3$ was mixed with 4ml OA, 6ml of OL-Am and 2 ml of pre-made oleylamine capped Ag NPs[16] (Figure S1) in a three-necked round bottom flask under vigorous stirring. This mixture was degassed at 110 °C for 30 mins followed by heating it up to 300 °C under inert atmosphere. This was kept at this temperature for another 30 mins before removing the heating mantle and cooling it down to room temperature. The as-synthesized Ag-Fe_3O_4 dimer was precipitated by ethanol, centrifuged at 5500 rpm for 3 mins. The precipitated product was re-dispersed in $CHCl_3$ for a repeated washing with ethanol/ $CHCl_3$ (v/v 1:4) until a clear supernatant liquid is obtained. At last, Ag-Fe_3O_4 dimer (Figure S2) was dispersed in 2 ml of $CHCl_3$.

Synthesis of Fe_3O_4-Ag_2S

The hybrid heterodimer of Ag_2S-Fe_3O_4 (Figure S3) was prepared by means of *in-situ* sulfurization of Ag-Fe_3O_4. To begin with, the S precursor was typically prepared by mixing 24.5 mg of elemental S with 5 ml of OL-Am and 2.5 ml of OA. This mixture was then degassed and left under vacuum at 90 °C for 30 mins to ensure the complete dissolution of S precursor. The previously prepared Ag-Fe_3O_4 dimer, in 2ml $CHCl_3$, was injected into the S solution under an N_2 blanket at room temperature and was left under continuous stirring for 1 hr. The obtained NPs were washed and purified by ethanol and $CHCl_3$ before re-dispersing it into 2 ml of $CHCl_3$.

Synthesis of Fe_3O_4-Ag_2S-ZnS

The trimer of ZnS-Ag_2S-Fe_3O_4 was synthesized by a sequential seeded-growth approach where Ag_2S-Fe_3O_4 was used as seed for the heterogeneous nucleation of ZnS. Zn oleate precursor was generated *in-situ* by mixing 42 mg of $Zn(NO_3)_2.6H_2O$ with 5ml of OA in a three-necked round bottom flask. After degassing, the solution was heated to up to 250 °C and was left at this temperature for 30 mins to allow the complete formation of Zn-oleate (colourless solution) before bringing it down to 100 °C. In a separate flask, 2 ml of the previously synthesized Ag_2S-Fe_3O_4 seed was mixed with 6 ml of ODE and 613 µL of DDT. The seed solution was injected into the Zn precursor solution at 100 °C. The temperature was subsequently increased to up to 220 °C and was left at this temperature for 5 mins. The final product was precipitated and purified by repeated washing with ethanol and $CHCl_3$. After drying of the sample, a yield of 32.7 mg was obtained.

Characterization

Transmission electron microscopy (TEM), High angle annular dark field-scanning TEM (HAADF-STEM), elemental mapping images and energy dispersive X-ray spectroscopy (EDS) were obtained from a FEI Talos F200X-FEG TEM at the John de Laeter Centre, Curtin University. The powder X-ray diffraction (XRD) pattern was collected on a D8 Advance (Bruker AXS, Germany) with Cu Kα radiation source at 40 KV/40 mA with a LynxEye detector and the X-ray photoelectron spectroscopy (XPS)

measurements were performed on a Kratos AXIS Ultra DLD at the John de Laeter centre, Curtin University.

Results and discussion

Herein, the formation of a hybrid heterotrimer of Fe_3O_4-Ag_2S-ZnS is a result of a well-known synthesis approach i.e. the seeded-growth method. In a two-step process, Fe_3O_4-Ag_2S dimer was prepared to be later on used as a seed for the growth of ZnS on the Ag_2S domain as a third entity (Figure S3). After the injection of seed, ZnS was allowed to heterogeneously nucleate for 5 mins onto the surface of Ag_2S at elevated temperatures i.e. 220 °C. Figure 1 presents the schematic illustration of this process.

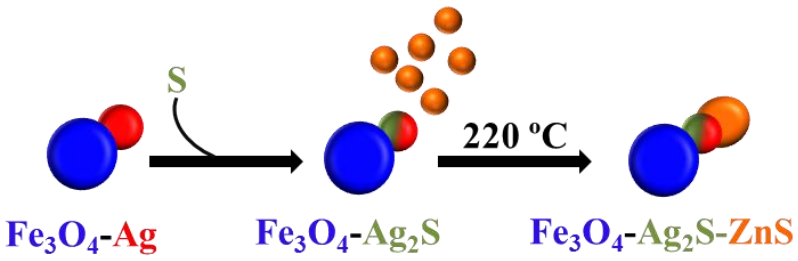

Figure 1. Stepwise schematic representation of the formation of Fe_3O_4-Ag_2S-ZnS.

It is worth mentioning here that the incoming ZnS entity preferred to nucleate on the surface of Ag_2S rather than Fe_3O_4 even though both of the domains were equally exposed. This could be attributed to the high affinity of ZnS monomers with the sulphur containing Ag_2S domain and the low lattice mismatch between the $(\bar{1}21)$ face of Ag_2S and the (200) face of ZnS i.e. 3.91 %.

Morphological and structural characterization

The TEM (Figure 2a) and HAADF-STEM (Figure 2b) shows the successful integration of three different functionalities in a single construct. The inset in Figure 2(a) shows the TEM image of original seed i.e. Fe_3O_4-Ag_2S. From the TEM image, it is difficult to identify three domains separately. Therefore, half circles of different colours were used to mark each entity separately i.e. cyan, red and orange for Fe_3O_4, Ag_2S and ZnS respectively. It is quite evident from the microscopic characterization that not all of the heterodimers were converted into trimers (~77% conversion), which could be improved by optimizing the seed to Zn precursor ratio.[6]

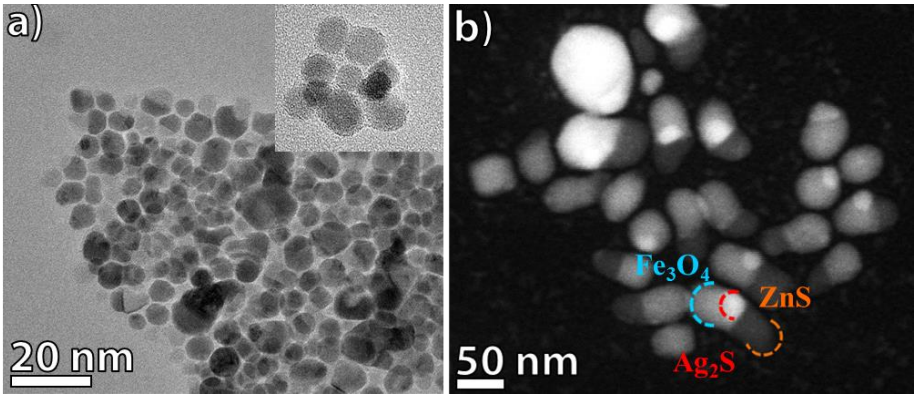

Figure 2. Microscopic characterization. (a) TEM and (b) HAADF-STEM image of Fe_3O_4-Ag_2S-ZnS trimer.

To confirm this further, elemental maps were obtained from the sample. Figure 3 not only verifies the co-existence of ZnS (Figure 3a) with the Fe_3O_4-Ag_2S dimer (Figure 3b-c) but also their corresponding locations.

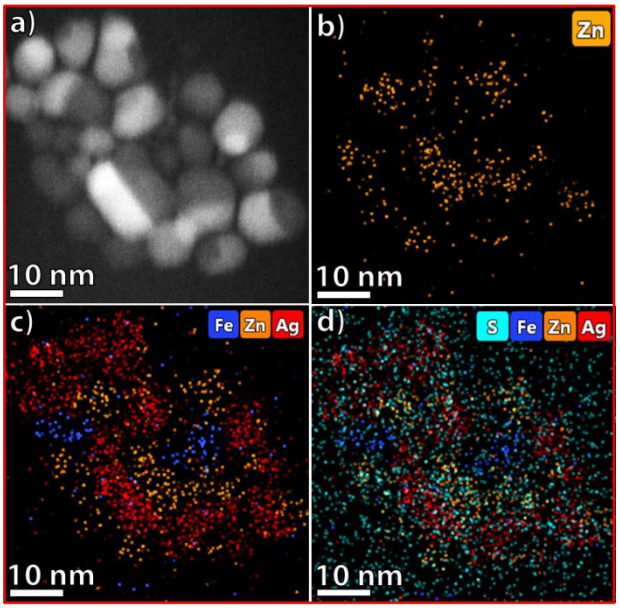

Figure 3. (a) HAADF-STEM image and elemental maps showing the distinct locations of (b) Zn (c-d) Fe, Ag and S in a complete map of Fe_3O_4-Ag_2S-ZnS trimer.

The EDS spectrum is provided in Figure 4 which affirms the presence of the above mentioned elements in the final trimer of Fe_3O_4-Ag_2S-ZnS.

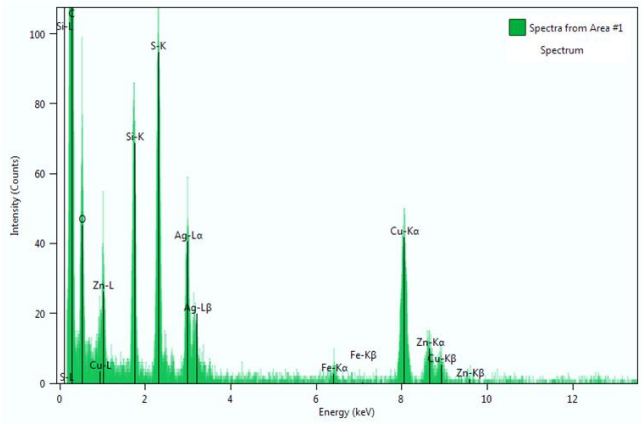

Figure 4. EDS spectra of Fe_3O_4-Ag_2S-ZnS corresponding to Figure 3.

The XRD pattern (Figure 5a) also displayed different sets of peaks which were found to be in good agreement with ZnS (cubic), Ag_2S (monoclinic) and Fe_3O_4 (cubic). The existence of typical diffraction peaks of ZnS at 28.558°, 33.089° and 47.515° provides a compelling evidence of the successful nucleation and growth of ZnS on Fe_3O_4-Ag_2S dimer. Some other characteristic peaks at 34.385° and 43.052° were attributed to the Ag_2S and face centred cubic Fe_3O_4 respectively. The size distribution analysis of a heterotrimer of Fe_3O_4-Ag_2S-ZnS (Figure 5b), shows its length in the range of 26.4±2.86 nm.

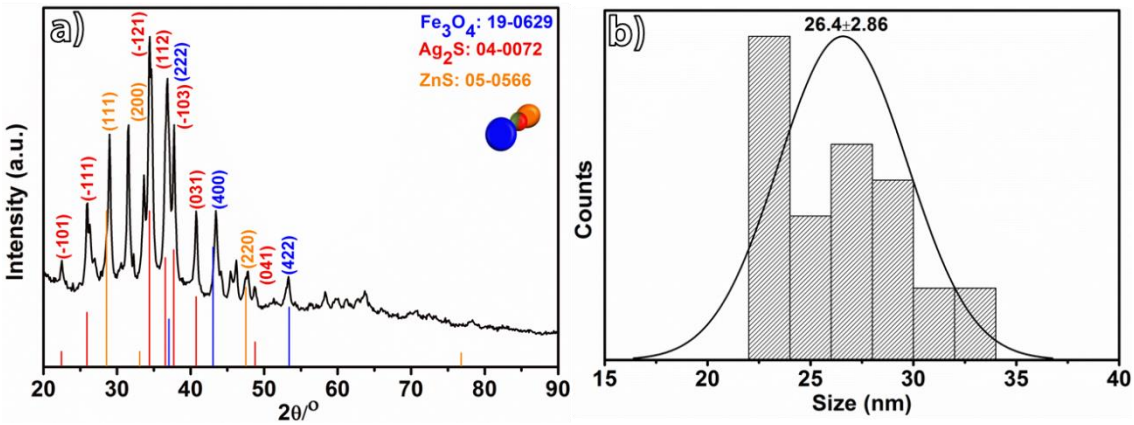

Figure 5. (a) XRD pattern and (b) size distribution curve of Fe_3O_4-Ag_2S-ZnS trimer.

The nature of chemical constituents and its valence states were analysed by XPS.[6] The survey spectra for dimer seed (Ag_2S-Fe_3O_4) and a trimer (ZnS-Ag_2S-Fe_3O_4) are shown in Figure 6. The appearance of the Zn peak at a binding energy of 1021 and 1045 eV (Figure 6b) verifies the successful incorporation of ZnS onto the dimer of Ag_2S-Fe_3O_4.[4] The signal of Fe in Fe_3O_4 was weak and could not be fitted appropriately. However, the appearance of oxygen peaks in both of the survey spectrum supports the presence of Fe_3O_4 in the sample. Also the high resolution O 1S spectra, shown in Figure S4, displays a peak at 530 eV which is typically associated with Fe-O.[23] The high resolution spectra of the most dominant and key components of the synthesized trimer (Figure 6b) are provided in Figure 6(c) i.e. Zn, Ag and S. It should be noted here that in the high resolution spectrum Zn, Ag and S (Figure 6c) contain doublet features which were assigned to Zn $2p_{3/2}$, Zn $2p_{1/2}$, Ag $3d_{3/2}$, Ag $3d_{5/2}$, S $2p_{½}$ and S $2p_{3/2}$ respectively.[24, 25] Additionally, the XPS spectrum of Zn 2p, Ag 3d and S 2p confirms their +2, +1 and -2 oxidation states respectively. Since the binding energy difference of these doublets matches well with the standard values, supporting the correct fitting and assignment of XPS peaks. Overall, Figure 5 (b-c) demonstrates that the reported trimer consist of ZnS, Ag_2S and Fe_3O_4 only.

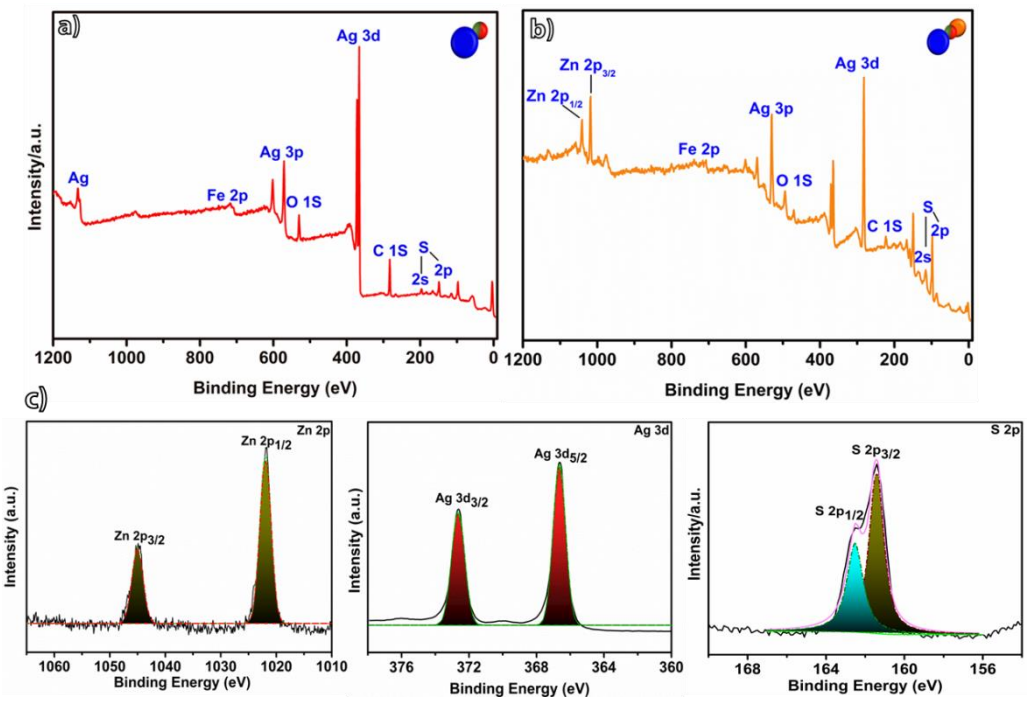

Figure 6. XPS survey spectra of (a) Fe_3O_4-Ag_2S (b) Fe_3O_4-Ag_2S-ZnS and its (c) high resolution spectra of Zn, Ag and S regions.

All of the above mentioned results obtained from TEM, XRD and XPS confirm the presence and exact location of individual constituents in the heterotrimer of Fe_3O_4-Ag_2S-ZnS. It also concludes the heterogeneous nucleation of incoming entity, ZnS, onto the Ag_2S domain rather than Fe_3O_4. Ongoing efforts are directed towards the implementation of this method towards other transition metal sulfides.

Conclusions

In conclusion, we have developed a relatively simple synthesis approach for the formation of a hybrid heterotrimer of Fe_3O_4-Ag_2S-ZnS. Thus was achieved by using a seeded-growth method, with well-defined morphology, conventionally not accessible by other methods. The growth of ZnS onto the Ag_2S domain of the Fe_3O_4-Ag_2S dimer was obtained under controlled experimental conditions. The availability of such trimers can be ideal candidates to open new avenues for the integration of other functionalities in a single-construct. The trimers of this nature holds promising applications for the energy related applications i.e. electro-photocatalytic hydrogen and oxygen evolution reactions, solar cells and batteries.[26]

Conflicts of Interest

The authors declare no conflicts of interest.

Acknowledgement

This project was supported by Australian Research Council (ARC) Discovery Early Career Researcher Award (DECRA) (Project ID: DE160100589). S.J. would like to acknowledge Curtin strategic international research scholarship (CSIRS). This research was undertaken by using the facilities (TEM, XRD and XPS) at the John de Laeter Centre, Curtin University. The authors also acknowledge the use of equipment, scientific and technical assistance of the WA X-ray Surface Analysis Facility, funded by the Australian Research Council LIEF grant LE120100026.

References

[1]. N. Waiskopf, Y. Ben-Shahar, U. Banin, *Adv. Mater.*, **2018**, *30*, 1706697. DOI:10.1002/adma.201706697.

[2]. U. Banin, Y. Ben-Shahar, K. Vinokurov, *Chemistry of Materials*. 2014;26(1):97-110. DOI:10.1021/cm402131n.

[3]. G. Jia, U. Banin, *J. Am. Chem. Soc*., **2014**,*136*, 11121. DOI:10.1021/ja505541q.

[4]. R. D. Amaranatha, R. Ma, M. Y. Choi, K. T. Kim, Appl. Surf. Sci., **2015**,324, 725. DOI:https://doi.org/10.1016/j.apsusc.2014.11.026.

[5]. W. Jiang, Z. Wu, X. Yue, S. Yuan, H. Lu, B. Liang, *RSC Adv*., **2015**, 5, 24064. DOI:10.1039/C4RA15774E.

[6]. S. Javaid, Y. Li, D. Chen, X. Xu, Y. Pang, W. Chen, F. Wang, Z. Shao, M. Saunders, J.-P. Veder, G. Jia, F. Jones, J. Phys. Chem. C, **2019**,*123*,10604. DOI:10.1021/acs.jpcc.8b11701.

[7]. Q. Chen, J. Song, C. Zhou, Q. Pang, L. Zhou, *Mater. Sci. Semicon. Proc*., **2016**, *46*, 53. DOI:http://dx.doi.org/10.1016/j.mssp.2016.02.005.

[8]. Z. G. Mohammadi, M. Malmir, N. Lashgari, A. Badiei, RSC Adv., **2019**, *9*, 25094. DOI:10.1039/C9RA01589B.

[9]. J. M. Hodges, R. E Schaak, *Acc. Chem. Res.*, **2017**, *50*, 1433. DOI:10.1021/acs.accounts.7b00105.

[10]. J. L. Fenton, B. C. Steimle, R. E. Schaak, *J. Am. Chem. Soc*., **2018**,*140*, 6771. DOI:10.1021/jacs.8b03338.
[11]. T. R. Gordon, R. E. Schaak, *Chem. Mater*., **2014**, *26*, 5900. DOI:10.1021/cm502396d.
[12]. M. J. Bradley, A. J. Biacchi, R. E. Schaak, *Chem. Mater*., **2013**, *25*, 1886. DOI:10.1021/cm4005163.
[13]. S. Liu, S. Guo, S. Sun, X.-Z. You, *Nanoscale*, **2015**, *7*, 4890. DOI:10.1039/C5NR00135H.
[14]. J. M. Hodges, J. R. Morse, M. E. Williams, R. E. Schaak, *J. Am. Chem. Soc*. **2015**, *137*,15493. DOI:10.1021/jacs.5b10254.
[15]. S. Javaid, X. Li, F. Wang, W. Chen, Y. Pang, S. Wang, G. Jia, F. Jones, J. Mater. Chem. C, [10.1039/C9TC03538A]. **2019**, DOI:10.1039/C9TC03538A.
[16]. J. M. Hodges, J. R.Morse, J. L. Fenton, J. D. Ackerman, L. T. Alameda, R. E Schaak, *Chem. Mater*., **2017**, *29*, 106. DOI:10.1021/acs.chemmater.6b02795.
[17]. S. Chandrasekaran, L. Yao, L. Deng, C. Bowen, Y. Zhang, S. Chen, Z. Lin, F. Peng, P. Zhang, *Chem. Soc. Rev.,* **2019**, *48*, 4178. DOI:10.1039/C8CS00664D.
[18]. R. C. Ghosh, S. Paria, *J. Phys. Chem. C*, **2013**,*117*,23385. DOI:10.1021/jp408105m.
[19]. S. Shen, Y. Zhang, L. Peng, Y. Du, Q. Wang, *Angew. Chem. Inter. Ed*., **2011**, *50*, 7115. DOI:10.1002/anie.201101084.
[20]. S. Singh, J. Chaturvedi, S. Bhattacharya, *RSC Adv*., **2014**, *4*, 11469. DOI:10.1039/C3RA48025A.
[21]. F. Pang, R. Zhang, D. Lan, J. Ge, *ACS Appl. Mater. Interfaces*, **2018**, *10*, 4929. DOI:10.1021/acsami.7b17046.
[22]. W. Shi, H. Zeng, Y. Sahoo, T. Y. Ohulchanskyy, Y. Ding, Z. L. Wang, M. Swiart, P.N. Prasad, *Nano Lett*., **2006**, *6*, 875. DOI:10.1021/nl0600833.
[23] X. Wang, Y. Liu, H. Arandiyan, H. Yang, L. Bai, J. Mujtaba, Q. Wang, S. Liu, H. Sun, *Appl. Surf. Sci.*, **2016**, *389,* 240. DOI: 10.1016/j.apsusc.2016.07.105
[24]. H. Abdullah, D.-H., Kuo, *ACS Appl. Mater. Interfaces*, **2015**, *7*, 26941. DOI:10.1021/acsami.5b09647.
[25]. G. Wang, Z. Li, M. Li, C. Chen, S. Lv, J. Liao, *Sci Rep*., **2016**, *6*, 29470. DOI:10.1038/srep29470.
[26] D. Chen, H. Zhang, Y. Li, Y. Pang, Z. Yin, H. Sun, L.-C. Zhang, S. Wang, M. Saunders, E. Baker, G. Jia, *Adv. Mater.*, **2018**, *30*, 1803351. DOI: 10.1002/adma.201803351

Table of content (Graphic)